Mine Closure 2025 – S Knutsson, AB Fourie & M Tibbett (eds)

doi:10.36487/ACG_repo/2515_96

Water quality and potential sources in alluvial bore, downstream of the tailings storage facility, Oyu Tolgoi copper mine, Mongolia

Tamir Puntsag [a,*], Samdanjigmed Tulganyam [a], Otgonbaatar Sededpurev [a], Sod-Erdene Bazardorj [a], Batdemberel Bayanzul [a], Bilguun Myagmar [b], Tamir Sarangerel [a], Altantungalag Danzan [a], Munkhtuya Natsagdorj [a], Purevsuren Nyambuu [a]

[a] *Oyu Tolgoi LLC, Mongolia*

[b] *Water Management LLC, Mongolia*

Abstract

Understanding water pathways and salinity transformations associated with tailings storage facilities (TSFs) is critical for long-term groundwater protection and effective mine closure planning, particularly in arid regions such as Mongolia's South Gobi region. This study examines increasing total dissolved solids (TDS) observed in shallow alluvial monitoring bore OTMB16-79, located downstream of the Oyu Tolgoi (OT) TSF. Isotope-based ($\delta^{18}O$, $\delta^{2}H$, $\delta^{34}S$, $^{87}Sr/^{86}Sr$) and elemental analyses (major, trace, and rare earth elements) were applied to distinguish TSF seepage from natural geochemical processes, including evaporative concentration, bedrock weathering, and displaced groundwater. Parameters such as $\delta^{34}S$, $^{87}Sr/^{86}Sr$, Na, and Cl were identified as key geochemical signatures for source differentiation. Results indicate that direct TSF seepage contributes less than 10% to the salinity at OTMB16-79, while approximately 31% originates from water collected and returned by the French drain system. These findings demonstrate the value of multivariate geochemical and isotopic tools in identifying source contributions and support the refinement of OT's conceptual hydrogeological model. The outcomes will contribute to establishing a risk-informed monitoring system and help prevent seepage migration, thereby supporting more effective and optimal TSF management.

Keywords: *total dissolved solids, tailings storage facility seepage, strontium, d-excess value, sulphur isotope*

1 Introduction

Understanding water pathways and transformations related to tailings storage facilities (TSFs), including potential seepage and subsurface migration, is essential for evaluating long-term risks to groundwater quality. This is particularly relevant for mine closure planning in semi-arid environments such as the South Gobi region of Mongolia, where the Oyu Tolgoi (OT) copper mine operates, A well-developed conceptual hydrogeological model plays a critical role in supporting responsible closure strategies and ongoing environmental protection. OT relies entirely on the Gunii Khooloi (GH) aquifer system, a confined deep groundwater source hosted within upper Cretaceous sedimentary formations and sealed by low-permeability layers that limit recharge and vertical connectivity with shallow aquifers. The aquifer's spatially variable thickness and transmissivity, combined with structural complexity (Tuvdendorj et al. 2008), make effective water management critical for both operations and closure.

OT recycles approximately 86% of its process water and uses just 0.4 m^3 per tonne of ore processed, demonstrating highly efficient water use within the mining industry (Oyu Tolgoi LLC 2024). A key contributor to this performance is the TSF integrated seepage collection system, which recovers water and helps protect surrounding aquifers from potential contamination.

* Corresponding author. Email address: tamirpu@ot.mn

Although the system remains largely effective, recent data provided by the London Mining Network (2024) indicates a gradual increase in salinity in some downstream alluvial monitoring bores adjacent to the TSF. This has raised questions regarding the sources and mechanisms contributing to changes in groundwater chemistry, particularly with respect to potential TSF seepage and natural geochemical processes such as evaporite dissolution and bedrock weathering (Clark & Fritz 1997). In the Gobi environment, high evaporation rates further intensify chemical changes in seepage water, complicating the interpretation of its origin and behaviour.

Although a comprehensive water monitoring program is in place and data are routinely shared with regulators and stakeholders, concerns persist regarding the long-term sustainability of groundwater use and the potential cumulative impacts on regional hydrogeological systems. By evaluating the effectiveness of current monitoring practices and identifying key salinity pathways, this study contributes to improved conceptual hydrogeological models and supports the development of targeted, risk-informed strategies for responsible mine closure aligned with approaches adopted at the Rio Tinto sites (Remy et al. 2024).

A gradual increase in total dissolved solids (TDS) at shallow alluvial monitoring bore OTMB16-79, located downstream of the TSF, prompted internal investigations by OT, identifying the seepage collection area as the likely source. A hydrogeochemical assessment (Matthew & Cecilia 2020) identified water sources contributing to surface seeps, explained increased solute concentrations in monitoring bores near the TSF, and described related environmental risks. Elevated TDS levels are attributed to seepage bypassing the Dyke via the pump station inlet pipe, upward displacement of groundwater, TSF seepage, evaporative concentration, and bedrock-driven flow paths. This study aims to evaluate the potential sources and migration pathways of increasing TDS in the alluvial aquifer near the TSF by applying isotope-based methods – specifically $\delta^{18}O$, $\delta^{2}H$, $\delta^{34}S$, and $^{87}Sr/^{86}Sr$ – alongside major, trace, and rare earth element analysis, following isotope-based approaches described by Nisi et al. (2014). The primary objective is to confirm whether the elevated TDS observed in shallow alluvial bore OTMB16-79 is attributable to TSF-related seepage, and if so, to quantify the contributions from various potential sources including displaced natural groundwater, TSF seepage, evaporative concentration, and upward migration of deep mineralised water through weathered bedrock. By characterising the chemical and isotopic signatures of these sources, the study aims to delineate salinity migration pathways within the complex hydrogeological system and better understand associated environmental risks.

2 Methodology

2.1 Sample collection and hydrogeological context

A total of 75 water samples were collected along the mine's water pathway, beginning at the water supply borefields of the GH and continuing through the processing circuit – including process water, thickener overflow, barge pond, and seepage collection ponds (referred to as seepage combined) – and extending to downstream monitoring bores located east of the TSF (Figure 1). In addition, a sample was collected from the French drain system installed below the Dyke cutoff, which intercepts residual shallow alluvial groundwater (≤0.6 L/s) and routes it to the seepage collection sump pond. Precipitation samples were also collected to characterise atmospheric inputs and support isotope-based evaluations of evaporation and recharge processes.

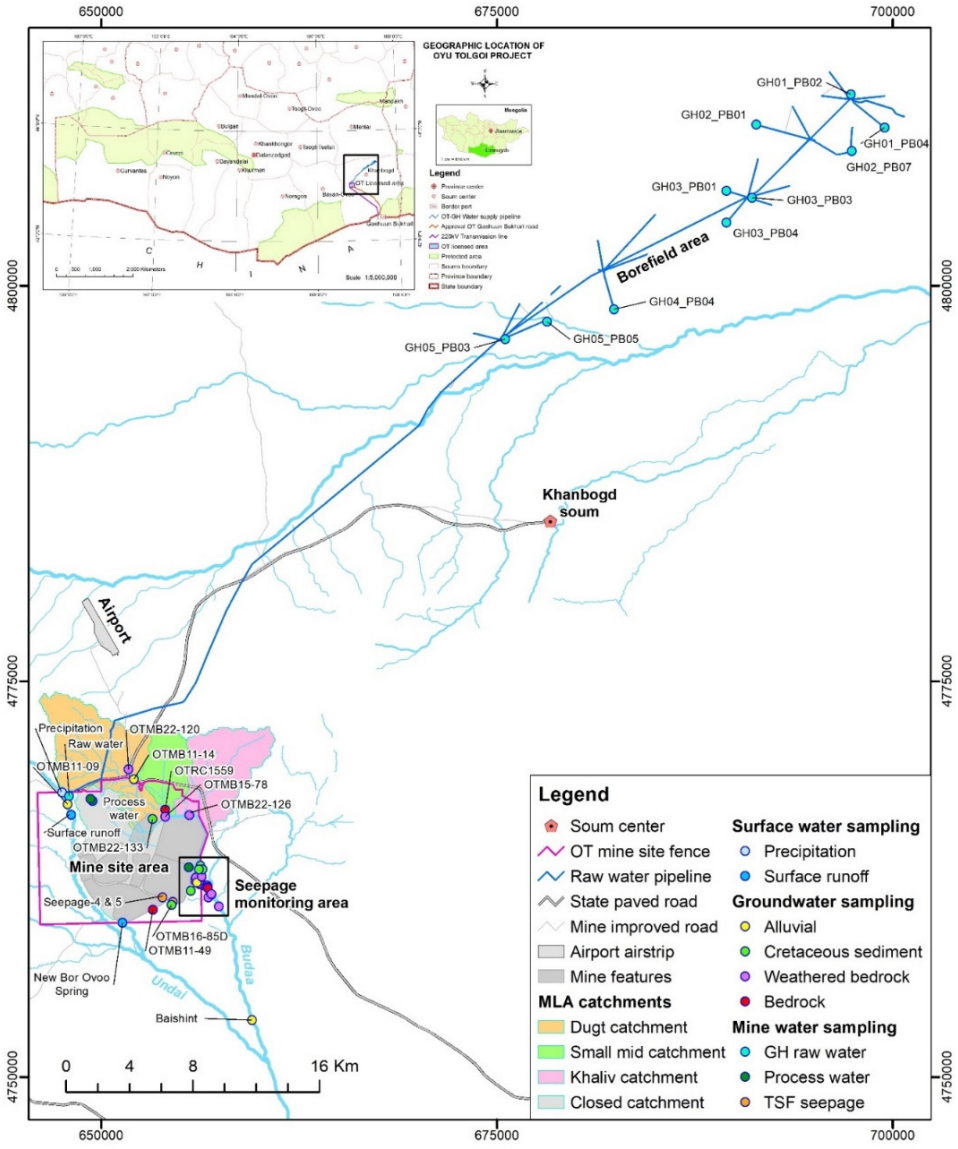

Figure 1 Study area and sampling locations of the Oyu Tolgoi mine site

Groundwater samples were collected from a range of monitoring boreholes situated in the vicinity of the TSFs, targeting key hydrostratigraphic units including surrounding alluvial deposits, weathered bedrock, and Cretaceous sediment zones. Borehole selection was based on long-term salinity trends, proximity to TSF infrastructure, and hydrogeological relevance to ensure representative coverage of the subsurface environment. The Budaa catchment, where the TSF is located, is underlain by low-permeability bedrock. The eastern portion is predominantly granite, while the western portion comprises a mix of intrusive rocks (quartz monzodiorite), volcanic units (andesite, tuffs), and sedimentary formations (sandstone and conglomerate). In the mine area, a variable thickness cover of Cretaceous clay (ranging from 5–30 m) overlies the bedrock, often containing thin interbedded sand layers and a basal gravelly-sand horizon. While Quaternary-age aeolian and fluvial sediments occur basin-wide, hydrological control is primarily governed by linear sand and gravel deposits associated with ephemeral stream channels.

The sampling strategy was designed to capture spatial variability in groundwater chemistry and identify areas where flow paths and geochemical mixing may occur, potentially influenced by evaporation or anthropogenic inputs such as TSF seepage. Spatial trends in TDS are used to qualitatively illustrate salinity variation across the site. Higher TDS concentrations were observed near infrastructure such as the TSF and French drain, helping to identify areas for further investigation (Figure 2).

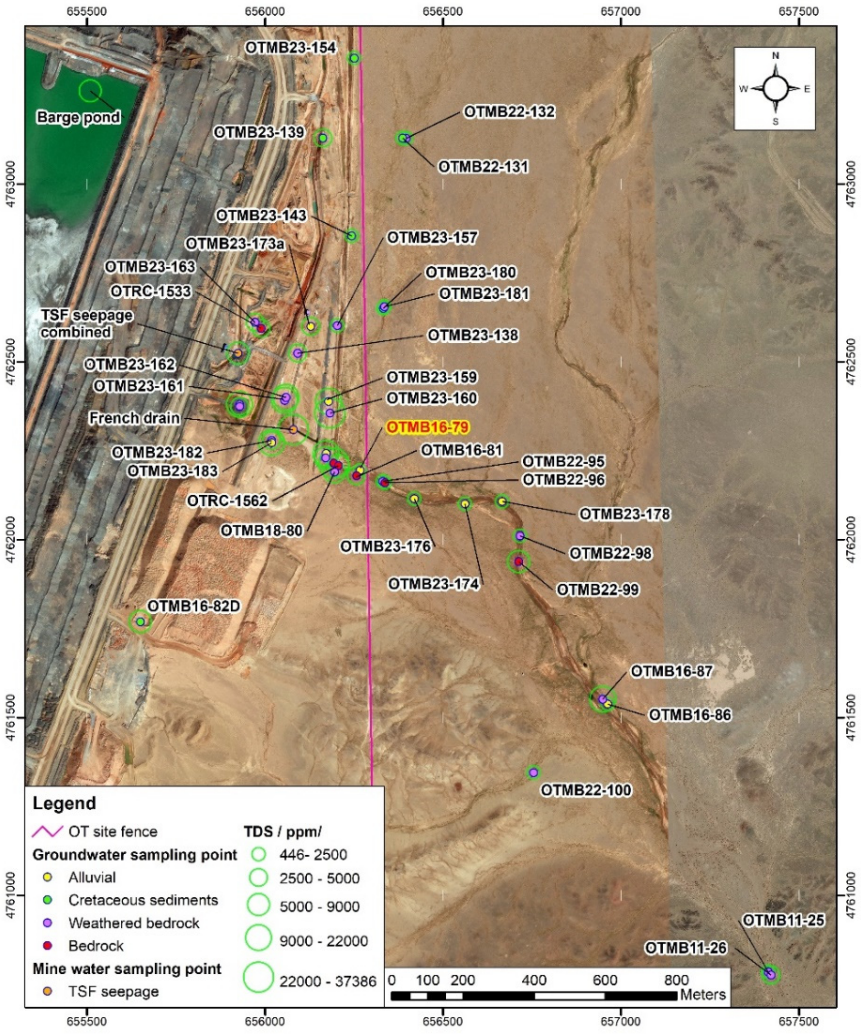

Figure 2 Total dissolved solids distribution near the tailings storage facility

While no definitive interpretations are presented at this stage, these patterns support the selection of focus areas for more detailed geochemical and hydrogeological assessments.

2.2 Sample preparation and analyses protocol

Water samples were collected in 15 mL glass vials (for hydrogen and oxygen isotopes), 50 mL pre-cleaned high density polyethylene (HDPE) vials (for strontium and boron isotopes), and 250 mL HDPE bottles (for sulphur isotope), including blanks and random duplicates with appropriate storage conditions maintained during shipment, as directed under analytical services provided by the West Australian Biogeochemistry Centre and the ICP-MS laboratory at the Centre for Microscopy, Characterisation and Analysis. The analytical program focused on determining trace element (TE) and rare earth element (REE) concentrations, along with stable isotope compositions (δ^2H, $\delta^{18}O$, $\delta^{11}B$, $^{87}Sr/^{86}Sr$, and $\delta^{34}S$). These parameters serve as sensitive geochemical tracers for identifying mixing processes, water-rock interactions, and potential anthropogenic influences. TE and REE concentrations support the interpretation of isotopic data and enhance the ability to distinguish between background groundwater chemistry and possible impacts from tailings seepage.

- TE and REE analysis: sample aliquots were centrifuged to remove particulates, and resulting supernatant was acidified with high purity nitric acid for analysis. Prior to isotopic analysis, samples were analysed for trace metals and REEs using a Thermo Element XR sector field mass spectrometer. Measurements were calibrated against National Institute of Standards and Technology, USA-NIST-certified standards.

- Stable hydrogen and oxygen Isotope: samples were analysed using a Picarro 2130i isotopic liquid water analyser and normalised to the Vienna standard mean ocean water (VSMOW) scale based on three laboratory standards calibrated against International Atomic Energy Agency (IAEA) reference materials (VSMOW2, standard light Antarctic precipitation (SLAP2), Greenland ice sheet precipitation (GISP)). Each was measured six times, with the first three runs discarded to minimise instrument memory effects. Analytical uncertainty was <0.50 ‰ for δ^2H and <0.05 ‰ for $\delta^{18}O$.
- Stable sulphur isotope: $\delta^{34}S$ values were expressed in per mil (‰) relative to the Vienna–Canyon diablo troilite scale, following the delta notation by Brand et al. (2014). Multi-point normalisation was applied using IAEA reference materials: IAEA-S1 (−0.30 ‰), IAEA-S2 (+22.62 ‰), IAEA-S3 (−32.49 ‰), and NBS127 (+21.12 ‰), as recommended by Brand et al. (2014) and Krouse & Coplen (1997). Analytical uncertainty was ±0.30 ‰ (1σ). Analyses were conducted using a Sercon 20-22 isotope ratio mass spectrometer coupled with an elemental analyser (SERCON, UK).
- Strontium isotope: approximately 0.2 µg of Sr was obtained by evaporating acidified samples at 120°C. After drying, 500 µL of high purity 3M HNO_3 was added. Sr purification was conducted using 50–100 µL of pre-cleaned Eichrom Sr-specific resin, conditioned with 3M HNO_3, following the method of Philip et al. (1992). The sample was loaded in 0.5 mL of 3M HNO_3, and the matrix was eluted using 2 mL of the same acid. The purified Sr fraction was diluted in 2% HNO_3 to ~30 µg/L. Isotope ratios were measured using a Thermo Neptune MC-ICP-MS with an Apex Omega desolvator. Measurements were made in static mode for 50 cycles (4.194 seconds each), and results were blank corrected for Sr and Kr backgrounds.^{87}Rb interference was corrected using $^{85}Rb/^{87}Rb$ =2.59265 (Steiger & Jäger 1977). Mass bias was corrected using the exponential law with a natural $^{86}Sr/^{88}Sr$=of 0.1194 (Russell et al. 1978), and external normalisation was performed using NIST SRM 987 ($^{87}Sr/^{86}Sr$ = 0.710249) in an article by Avanzinelli et al. (2005). Procedural blanks and NIST SRM 987 were analysed in replicate, showing precision better than ±0.00002 (2σ).
- Boron isotope: a 400 µL of each sample was purified using sequential cation (Bio-Rad AG50W-X8) and anion (Bio-Rad AG1-X8) exchange resins, following McCulloch et al. (2014). The purified B fraction was diluted in 2% HNO_3 and analysed using a Neptune Plus MC-ICPMS with AE121 bracketing ($\delta^{11}B$ = 19.81‰). Measurements precision was ±0.08‰ (2SE, n = 75), with AE121 repeatability of ±0.01‰ (σ, n= 43). External standards showed of 0.3‰ (σ, n = 7) precision, and column recovery tests confirmed no statistically significant bias (0.13 ± 0.19‰ (σ, n = 4).

3 Data

3.1 Hydrochemical baseline data

Baseline hydrochemical data for most monitoring bores has been available since 2016. Groundwater in the deeper Cretaceous sequence, interstitial sands and gravels, and bedrock is generally brackish and slightly basic, while groundwater from surficial formations remains relatively fresh (TDS < 1,000 mg/L). pH is typically alkaline, ranging mostly between 8 and 9, and remains stable at nearly all monitoring locations. Figure 3 presents a trinary piper plot characterising major ions from all aquifers based on historical monitoring data, along with samples collected from the current isotopic and trace metals study.

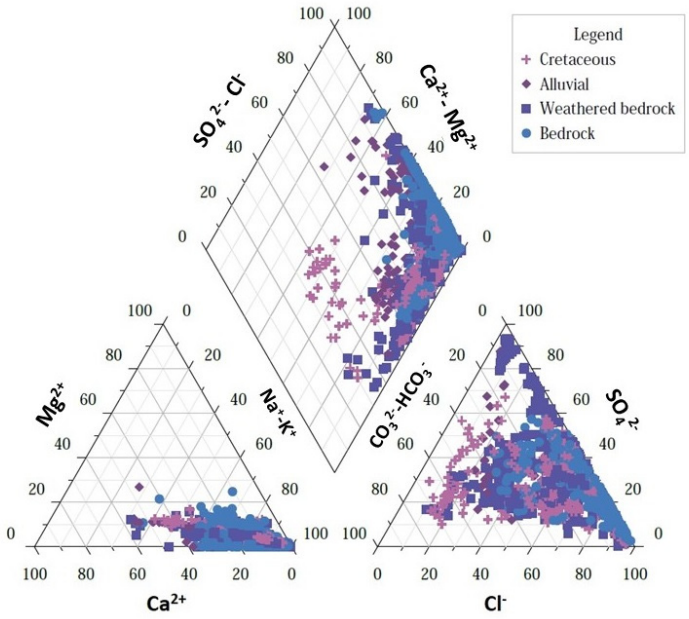

Figure 3 Ternary piper plot depicting major ion characterisation of the assets of monitoring bores

The diagram highlights clear geochemical distinctions between the four aquifer types. Water from the Cretaceous and alluvial aquifers shows greater variability, suggesting influence from evaporative processes or TSF seepage. In contrast, the weathered bedrock and bedrock aquifers exhibit more consistent chemistry, indicating limited interaction with surface or anthropogenic sources. The overall major ion composition of groundwater suggests it is the Na-Cl type, with minor variations in Ca, and Mg and carbonate concentrations. These findings emphasise the vulnerability of shallow aquifers and underscore the need for targeted monitoring and aquifer-specific management approaches in mine closure planning.

Figure 4 plots the SO_4^{2-}/Cl^- and K^+/Mg^{2+} ratios to show differences between process water and various field samples.

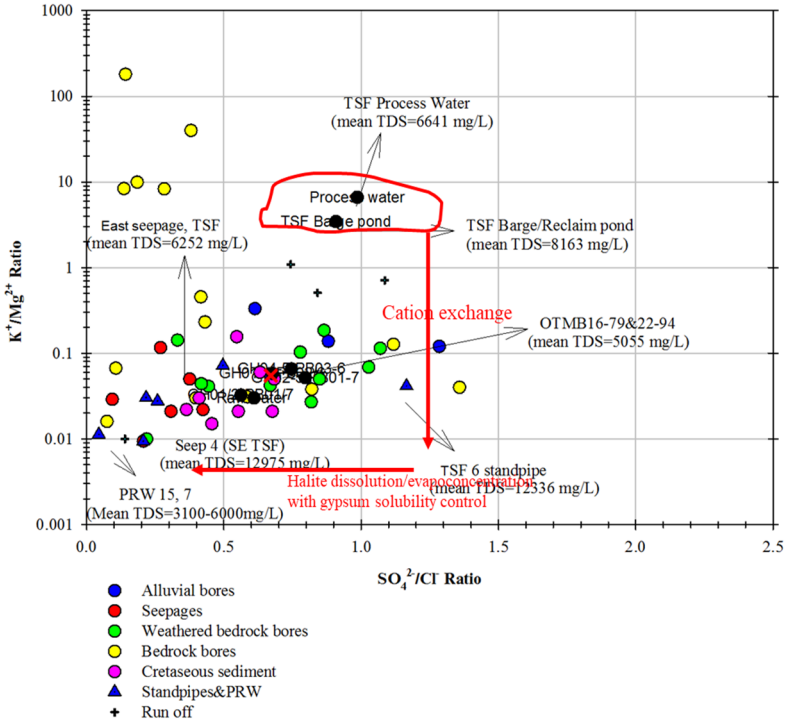

Figure 4 Relationships between the potassium (K), magnesium (Mg) and sulphate to chloride ion ratios

These ratios serve as geochemical tracers to assess potential mixing and influence from TSF seepage. Process water samples exhibit clear patterns, with SO_4^{2-}/Cl^- ratios consistently above 1.0 and K^+/Mg^{2+} ratios exceeding 4, reflecting concentration from ore processing and evaporation. In contrast, seepage, alluvial, and Cretaceous aquifer samples mostly show ratios below 1.0, suggesting different geochemical characteristics and limited direct influence from process water. This distinction provides a critical baseline for ongoing monitoring and closure planning. Only selected chemical parameters are discussed here, focusing on those most relevant to the study's objectives and research questions.

3.2 Isotopic and trace elements data

This research investigated the spatial variation in groundwater quality using five stable isotopes ($\delta^{18}O$, δ^2H, $^{87}Sr/^{86}Sr$, $\delta^{11}B$, $\delta^{34}S$), 6 REE (La, Ce, Pr. Nd. Ho, Y) and 31 TE (Li, B, Rb, Sr, Y, Mo, Rh, Pd, Cd, Sn, Sb, Cs, W, Pb, Th, U, Na, Mg, Al, P, S, Cl, Ca, Ti, V, Mn, Fe, Co, Ni, Cu, Zn and Ba). The 75 samples exhibit a large variation in TE compositions, with the lowest concentrations observed in samples as precipitation and the highest concentrations typically found in groundwater samples.

The local meteoric water line (LMWL) for OT was derived from precipitation monitoring and is defined as $\delta^2H = 6.91\delta^{18}O - 12.7$. This is compared with the global meteoric water line (GMWL), $\delta^2H = 8.1\delta^{18}O + 10$ (Craig 1961). These reference lines are used later in the results section to interpret stable isotope data and assess evaporative effects and recharge sources. The isotopic composition also shows a broad range in snow and new precipitation samples after drought, with $\delta^{18}O$ values varying from -25.0‰ to -1.8‰ and δ^2H values ranging from -186‰ to -25.8‰. The isotopic composition also shows a broad range, with boron isotopes varying from 4.35‰ to 51.2‰, sulphur isotopes ranging from 1.4‰ to 13.6‰, and strontium isotopes ranging from 0.7059 to 0.7095.

To determine the water source contributions to OTMB16-79 using principal component analyses (PCA) and a linear mixing model based on geochemical and isotopic parameters. The PCA for the data has been performed using JMP Pro 16.2 (Milliken 2000). Then the mixed model was run more than 10 times, and each parameter was assigned a weight based on its importance for distinguishing sources using the JMP Pro 16.2.

4 Results

4.1 Exploratory data analysis

The Spearman rank-order correlation analysis was applied to the full 75 sample dataset to assess spatial relationships among water quality parameters. This method was selected for its suitability with non-normally distributed environmental data. Table 1 shows strong positive correlations among most trace elements, indicating similar geochemical behaviour or common sources. In contrast, stable isotopic values exhibit significant negative correlations with several chemical parameters, suggesting different controls or source influences on isotopic composition compared to trace elements. $\delta^{34}S$ values showed a significant negative correlation with most of the parameters, which indicated its influence on other indicators. The strongest correlation was observed Mo and Sb (correlation coefficient of 1), indicating linear predictability between these two parameters. A strong positive correlation of Ca^{2+} and Mg^{2+} with Na^+ (r^2adj = 0.87 and 0.74, respectively) indicates contributions from silicate weathering, halite dissolution, and other evaporites such as gypsum, calcite, fluorite, borates, and sodium carbonates, as noted in the hydrogeochemical assessment of water emergence at the TSF (Matthew & Cecilia 2020).

Table 1 Correlation matrix of groundwater quality parameters, bold indicates significant at 0.05 level

	$\delta^{18}O$	$\delta^{2}H$	$\delta^{34}S$	$\delta^{87}Sr$	Rb	Sr	Mo	Cd	Sb	Cs	Pb	Na	Mg	Cl	K	Ca
Ca	0.67	0.46	-0.72	-0.38	0.54	0.99	0.58	0.66	0.64	0.57	0.84	0.87	0.49	0.82	0.56	1.00
K	0.53	0.28	-0.92	-0.68	0.99	0.48	0.99	0.90	0.99	0.98	0.64	0.22	-0.41	0.06	1.00	
Cl	0.51	0.45	-0.30	0.08	0.04	0.85	0.07	0.21	0.14	0.06	0.63	0.97	0.84	1.00		
Mg	0.15	0.20	0.20	0.31	-0.43	0.58	-0.39	-0.21	-0.32	-0.39	0.33	0.74	1.00			
Na	0.61	0.53	-0.43	-0.02	0.18	0.88	0.23	0.38	0.30	0.23	0.69	1.00				
Pb	0.47	0.29	-0.65	-0.38	0.57	0.84	0.63	0.72	0.67	0.64	1.00					
Cs	0.53	0.27	-0.92	-0.69	0.95	0.49	0.99	0.96	0.99	1.00						
Sb	0.57	0.31	-0.95	-0.67	0.97	0.55	1.00	0.94	1.00							
Cd	0.55	0.30	-0.88	-0.63	0.84	0.60	0.92	1.00								
Mo	0.55	0.29	-0.93	-0.69	0.98	0.50	1.00									
Sr	0.62	0.41	-0.62	-0.38	0.45	1.00										
Rb	0.53	0.28	-0.92	-0.68	1.00											
$\delta^{87}Sr$	-0.19	0.10	0.49	1.00												
$\delta^{34}S$	-0.71	-0.47	1.00													
$\delta^{2}H$	0.94	1.00														
$\delta^{18}O$	1.00															

4.2 Evaporation characterisation using $\delta^{2}H$ and $\delta^{18}O$ values of water

Figure 5 shows the relationship between $\delta^{2}H$ and $\delta^{18}O$ isotopes of all samples and mixing Gunii Khooloi water reserve, process, barge and tailing water and natural waters of different hydrological units. The observed differences between mine tailing with the main water reserve suggests more evaporates than the natural waters. Samples from weathered bedrock and Cretaceous sediments plot slightly below the LMWL, suggesting some evaporative enrichment.

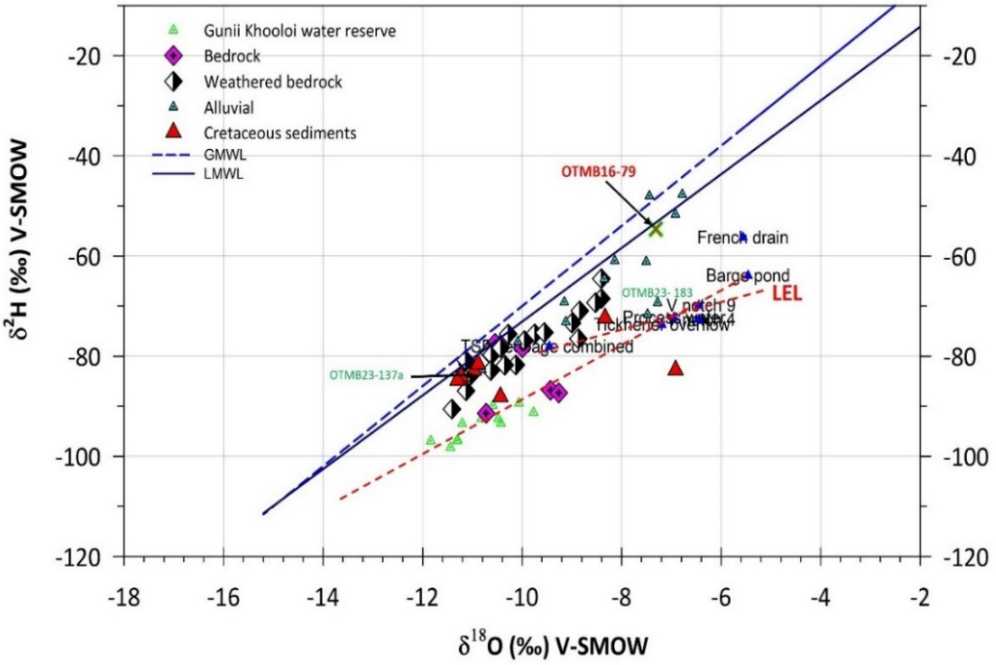

Figure 5 Plot of $\delta^{2}H$ and $\delta^{18}O$ for main water types of Oyu Tolgoi mine (LEL = local evaporation line; GMWL = global meteoric water line; LMWL = local meteoric water line)

Our study uses *d-excess* ($\delta^2H - 8 \times \delta^{18}O$) to trace water sources affected by evaporation and non-equilibrium processes such as diffusion and dissociation. Because evaporation lowers *d-excess* by preferentially removing lighter isotopes, lower values typically indicate stronger evaporative effects. According to Puntsag et al. (2016), in contrast, higher *d-excess* values reflect moisture from colder, drier climates with minimal evaporation. Based on the isotopic data, processing water types – including process water, barge pond water, thickener overflow, and seepage – exhibit lower *d-excess* values compared to deeper groundwater from monitoring bores. This pattern indicates that these waters have been more strongly influenced by evaporative processes.

4.2 Main sources and chemical signatures

PCA was initially applied to the full dataset, revealing that boron isotopes ($\delta^{11}B$) were positively correlated with major cations (Na^+, Mg^{2+}, Ca^{2+}), while strontium isotopes ($^{87}Sr/^{86}Sr$) were negatively correlated with trace elements including K^+, Rb, Cs, Mo, Cd, and Sb. Despite these associations, the first two principal components accounted for only 31% of the total variance, indicating that PCA alone did not adequately resolve the underlying geochemical relationships.

PCA was applied to 19 chemical variables, including isotopes ($\delta^{18}O$, δ^2H, d-excess, $\delta^{34}S$, $\delta^{11}B$, $^{87}Sr/^{86}Sr$) and major/minor elements (Rb, Sr, Mo, Cd, Cs, Pb, Na, Mg, Cl, K, Ca, Zn), from 75 groundwater, process water, and precipitation samples to identify key contributors, reduce dimensionality, and interpret geochemical patterns.

In Figure 6, PCA results showed that PC1 (52.5%) and PC2 (31.3%) together explained 83.8% of the total variance, effectively capturing the major geochemical variability within the dataset. In panel (a), the 11 grouped water types formed distinct clusters, allowing differentiation between key sources. Process-related waters such as thickener overflow and barge pond were associated with elevated concentrations of K, Mo, Cd, and Sb, while groundwater samples influenced by weathered bedrock and Cretaceous sediments correlated with lower $^{87}Sr/^{86}Sr$ ratios, $\delta^{34}S$, and *d-excess*. The bedrock-alluvial cluster shows elevated $\delta^{34}S$, $\delta^{11}B$, and $^{87}Sr/^{86}Sr$, indicating naturally derived origin from natural water-rick interaction with minimal TSF influence. Interestingly, OTMB16-79 plots near weathered bedrock and Cretaceous sediments, indicating a natural origin with no clear geochemical signature of direct TSF seepage.

Panel (b) of the PCA plot showed two main geochemical gradients and helped identify patterns among individual monitoring samples of upper part of OTMB16-79. Component 1 (66.3%) captured variability driven by metal concentrations (Cu, Zn) and major ions (K^+, Na^+, Cl^-), indicating a strong influence from TSF seepage. Component 2 (10.1%) reflected variation in isotopic compositions, particularly $\delta^{34}S$ and $^{87}Sr/^{86}Sr$, highlighting the role of sulphate-related processes and source differentiation. Based on sample clustering and variable associations, four distinct geochemical groups were identified. The TSF seepage group (OTMB16-79, OTMB23-137a, OTMB23-157) clustered near the “TSF seepage combined” centroid and was linked to elevated sulphate concentrations and strontium isotopic values, consistent with seepage water influence. The French drain group (OTMB23-161, OTMB23-155) showed elevated Ca, Mg, and Li, indicating a geochemical signature distinct from TSF influence, likely reflecting groundwater–drainage interactions. OTMB23-145 and OTMB23-183, classified as the High-metal group, were associated with trace metal enrichment, suggesting localised contamination or residual seepage effects. OTMB23-139, forming a sulphate-isotopic group, was characterised by strongly negative $\delta^{34}S$, suggesting input from natural or localised sulphate cycling.

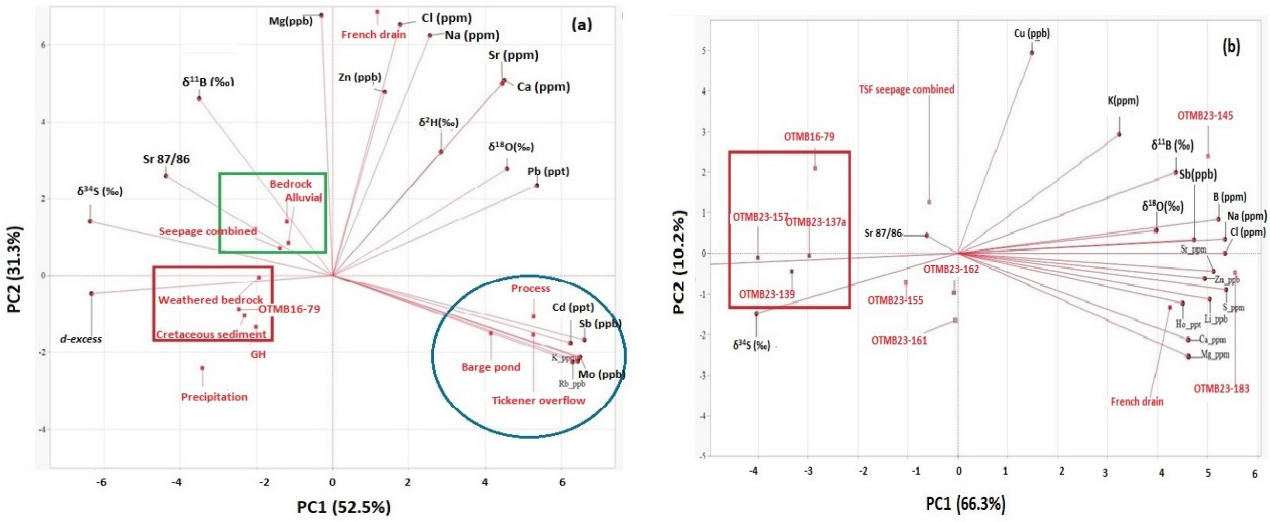

(a) (b)

Figure 6 Scatter diagram of (a) PC1 versus PC2 loadings of the main sources and (b) PC1 versus PC2 loadings of the nearby sources of OTMB16-79

The spatial and chemical proximity of these samples supports the interpretation that OTMB16-79 may be influenced by shallow sources with elevated $^{87}Sr/^{86}Sr$ ratio. Geochemical signatures linked to bedrock weathering reflected natural contributions, while potential overlap with TSF seepage may exist in certain zones. Additionally, samples from French drain and seepage areas exhibited mixed influences from industrial processes (e.g. elevated trace metals) and natural isotopic compositions, emphasising the need to differentiate mine-related impacts from natural background variability in long-term water quality assessments. OTMB23-183 was clearly separated from other groups in the PCA plot, showing elevated levels of Na^+, Mg^{2+}, Ca^{2+}, Cl^-, Zn, and Mo. Its isotopic composition indicated a mixed influence from natural and industrial sources. Its proximity to the process water group suggests possible impact from TSF seepage or infrastructure leakage. This sample is important for distinguishing mine-related effects from natural background conditions.

4.3 Potential source to OTMB16-79

A linear mixing model was used to estimate source contributions to OTMB16-79, assuming its composition reflects a weighted mix of TSF seepage, OTMB23-137a, OTMB23-157, OTMB23-183, OTMB23-139 and French drain samples. Parameters such as $\delta^{34}S$, $^{87}Sr/^{86}Sr$, Na, and Cl had the most influence on source differentiation and were assigned higher weights. In Table 2, the less informative parameters were removed based on field relevance and PCA support. Source samples used in the model were chemically distinct, avoiding overlap.

Table 2 Selected data and information for mixing model analysis

Sample name	OTMB16-79 (as mixture)	TSF seepage combined	French drain	OTMB23-137a	OTMB23-157	OTMB23-183	OTMB23-139
Distance (km)	0.5	0	0.2	0.2	0.3	0.38	0.2
Type	Alluvial	TSF seepage	TSF seepage	Alluvial	Weathered bedrock	Alluvial	Cretaceous sediments
Depth (m)	1.5			6	6.3	3.2	9
$\delta^{18}O$ (‰)	-7.3	-9.4	-5.6	-10.8	-11	-7.3	-11.3
d-excess	3.9	-2.5	-11.8	3.8	4.5	-11.1	5.6
$\delta^{34}S$ (‰)	7.2	6	6.9	7.8	7.4	5.6	7.5
$Sr^{87}/^{86}$	0.7092	0.7085	0.7087	0.7089	0.7084	0.7090	0.7092
Na_ppm	728	2,567	8,019	1,133	831	12,404	1,743
Cl_ppm	595	3,374	11,418	1,644	578	16,710	2,674
Cu_ppb	25.4	22.67	5.64	0	0.93	7.55	0.91
Zn_ppb	5.35	20.25	143	5.7	4.08	144	15

A mixed model analysis (with multiple variance components) was performed in JMP 5.1 using restricted maximum likelihood method. Least squares means were generated for each source to support F-statistics used in fraction calculations (Hummel et al. 2021).

Mixing model results for OTMB16-79 indicate a strong fit between observed and predicted values, with small residuals across all parameters (adjusted $R^2 = 0.91$, $P < 0.001$) as shown in Figure 7. Mixing model results for OTMB16-79 indicate a strong fit between observed and predicted values, with small residuals across all parameters (adjusted $R^2 = 0.91$, $P < 0.001$) as shown in Figure 6. The largest contributions were from OTMB23-183 (46%) and the French drain sump water (31%), suggesting that OTMB16-79 reflects a mixture of waters influenced by both localised groundwater conditions and infrastructure-related flows. Minor inputs were attributed to TSF seepage (9%), OTMB23-139 (7%), OTMB23-137a (5%), and OTMB23-157 (2%). These results confirm that OTMB16-79 is situated within a transitional zone where processed water pathways, seepage impacts, and natural geochemical backgrounds converge. The use of site-specific samples as end-members – rather than idealised group averages – strengthened the reliability of source attribution by capturing field-based variability. Overall, the analysis supports a robust interpretation of hydrochemical mixing, providing insights into the spatial distribution of source influences around the TSF.

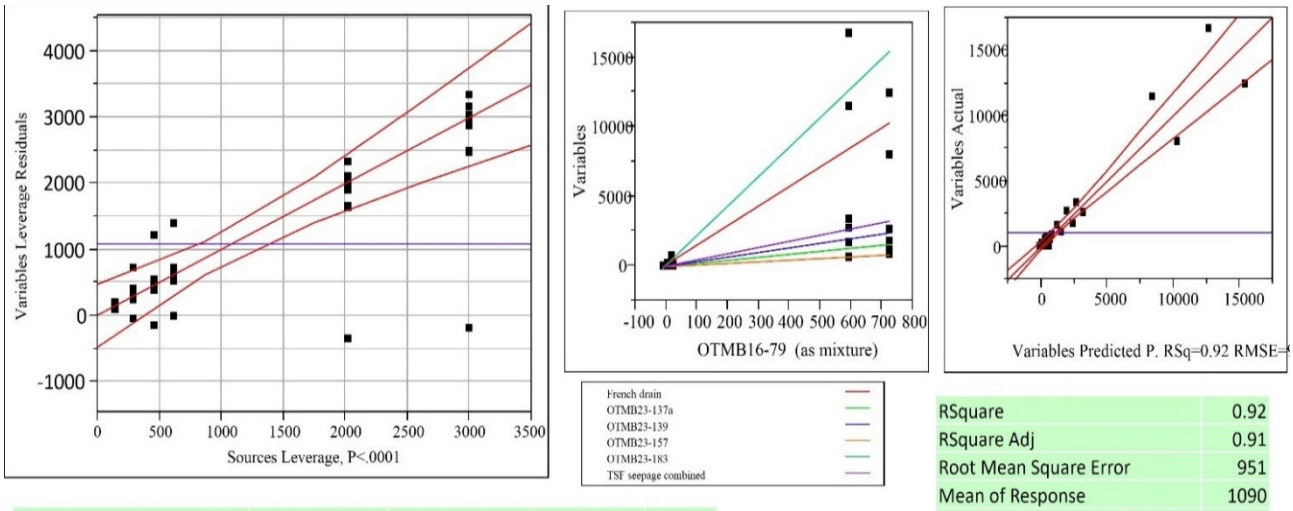

RSquare	0.92
RSquare Adj	0.91
Root Mean Square Error	951
Mean of Response	1090
Observations (or Sum Wgts)	60

Potential source	Least Sq Mean	Proportion to the mixture	%
French drain	2019	0.31	31
OTMB23-137a	296	0.05	5
OTMB23-139	459	0.07	7
OTMB23-157	144	0.02	2
OTMB23-183	3001	0.46	46
TSF seepage combined	619	0.09	9

Figure 7 Mixing model results for calculation of main sources to OTMB16-79

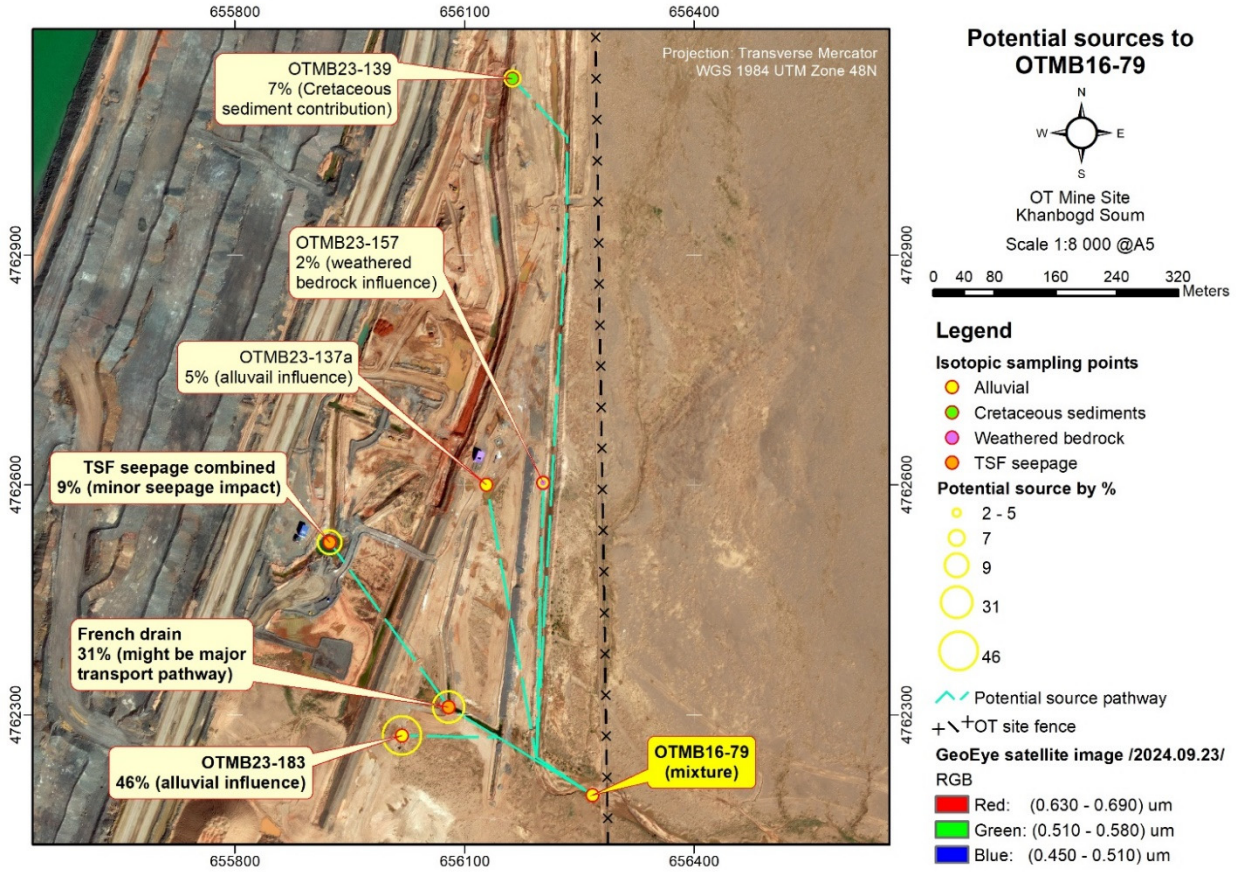

Figure 8 Main sources to the OTMB16-79

Mixing model results suggest that OTMB16-79 may receive contributions from multiple sources with varying geochemical signatures. OTMB23-183 appears to be a dominant source (up to 46%), possibly reflecting influence from deeper alluvial sediments. The French drain, contributing an estimated 31%, may act as a major transport pathway, collecting water from multiple depths and lithologies along its alignment. Additional minor influences are indicated from combined TSF seepage (9%), OTMB23-139 (7%, Cretaceous sediments), OTMB23-137a (5%, alluvial), and OTMB23-157 (2%, weathered bedrock).

OTMB23-139 and OTMB23-157 may be influenced by weathered bedrock and Cretaceous sediments, showing no clear geochemical signature of TSF seepage, while OTMB23-183, due to its shallow depth and elevated process-related indicators, reflects surface-level TSF seepage influence and is not representative of deeper aquifer conditions (Table 2). The spatial pattern of source points and interpreted flow paths, shown in Figure 8, supports the interpretation that OTMB16-79 lies within a hydrochemically mixed zone. The inferred mixing may result from interactions between infrastructure-related seepage pathways and naturally variable groundwater conditions. These findings provide preliminary insights into the complexity of source contributions, though further site-specific validation is recommended.

5 Conclusion

Multivariate geochemical and isotopic analyses suggest that OTMB16-79 reflects a mixture of water influenced by potential sources, including alluvial groundwater and infrastructure-related inputs, with limited TSF seepage contribution (<10%). Key geochemical and isotopic indicators, including $\delta^{34}S$, d-excess, Sr, and elements such as Cu, K, Na, Cl, and Zn, were essential in identifying dominant processes such as evaporative enrichment and mineral dissolution. Process-affected waters exhibited lower d-excess values compared to deeper monitoring bores, indicating stronger evaporative influence along industrial flow paths. The French drain was estimated to contribute approximately 31% as a potential source based on the mixing model, but its primary function is to collect seepage water from the surrounding area and return it to the mine's water recirculation system. This role is essential for controlling seepage migration and supporting efficient water re-use. This study focused on identifying the potential sources and flow pathways influencing the hydrochemistry of OTMB16-79. By applying multivariate geochemical and isotopic tools, it was possible to distinguish between natural and process-related influences. The findings enhance the current understanding of seepage dynamics and provide a strong foundation for designing targeted monitoring programs and supporting sustainable water management at the TSF.

Acknowledgement

This project was funded by Oyu Tolgoi LLC. We sincerely thank Greg Skrzypek and Aleksey Sadekov for conducting the isotopic and TE analyses, and Oyunzul Gantulga for leading the project contract and overseeing its implementation. We gratefully acknowledge the support and collaboration of the Water Team, Environment Department, Tailings and Hydrogeology team, as well as Rio Tinto's senior hydrogeologists and geochemists, for their valuable advice, technical input, and assistance throughout the sampling campaign. We also extend our thanks to the Travel and Finance teams at Oyu Tolgoi LLC for their essential contributions to the successful completion of this project.

References

Avanzinelli, R, Boari, E, Conticelli, S, Francalanci, L, Guarnieri, L, Perini, G, … Ulivi, M 2005, 'High precision Sr, Nd, and Pb isotopic analyses using the new generation Thermal Ionization Mass Spectrometer Thermo Finnigan Triton-Ti®', *Periodico di Mineralogia*, vol. 75, pp. 147–166.

Brand, WA, Coplen, TB, Vogl, J, Rosner, M & Prohaska, T 2014, 'Assessment of international reference materials for isotope-ratio analysis', *Pure and Applied Chemistry*, vol. 86, pp. 467–472.

Clark, I & Fritz, P 1997, *Environmental Isotopes in Hydrogeology*, CRC Press, Boca Raton.

Craig, H 1961, 'Isotopic variations in meteoric waters', *Science*, vol. 133, no. 3465, pp. 1702–1703.

Hummel, RM, Elizabeth, A, Claassen, RD & Wolfinger, RD 2021, *JMP® for Mixed Models*, SAS Institute Inc., Cary.

Krouse, HR & Coplen, TB 1997, 'Reporting of relative sulphur isotope-ratio data', *Pure and Applied Chemistry*, vol. 69, pp. 293–295.

London Mining Network 2024, *Rio Tinto: Get Serious About Addressing Community Harm*, viewed 13 April 2025, https://londonminingnetwork.org/2024/03/rio-tinto-get-serious/

Matthew, M & Cecilia, LS 2020, *Final Report: Hydrogeochemical Assessment of Water Emergence at the Tailings Storage Facility (TSF), Oyu Tolgoi (OT)*, prepared for Oyu Tolgoi LLC, Ulaanbaatar.

McCulloch, MT, Holcomb, M, Rankenburg, K & Trotter, JA 2014, 'Rapid, high-precision measurements of boron isotopic compositions in marine carbonates', *Rapid Communications in Mass Spectrometry*, vol. 28, pp. 2704–2712, https://doi.org/10.1002/rcm.7065

Milliken, GA 2000, 'Mixed models analysis using JMP® software 4.0', *Proceedings of the Twenty-Fifth Annual SAS Users Group International Conference*, SAS Institute Inc., Cary, pp. 276–282.

Nisi, B, Raco, B & Dotsika, E 2014, 'Groundwater contamination studies by environmental isotopes: a review', *Threats to the Quality of Groundwater Resources: Prevention and Control*, Springer, Berlin, pp. 115–150.

Oyu Tolgoi LLC 2024, *Independent Environmental and Social Consultant Audit Report: September 2024*, Oyu Tolgoi LLC, viewed 13 April 2025, https://admin.ot.mn/wp-content/uploads/IESC-Audit-Report_September_2024.pdf

Philip, HE, Chiarizia, R & Dietz, ML 1992, 'A novel strontium-selective extraction chromatographic resin', *Solvent Extraction and Ion Exchange*, vol. 10, pp. 313–336, https://doi.org/10.1080/07366299208918107

Puntsag, T, Mitchell, MJ, Campbell, JL, Klein, ES, Likens, GE & Welker, JM 2016, 'Arctic vortex changes alter the sources and isotopic values of precipitation in northeastern US', *Scientific Reports*, vol. 6, no. 22647.

Remy, M, Clode, K, Motchan, T & Kerr, H 2024, 'Water treatment development plan for Rio Tinto closure assets', in AB Fourie, M Tibbett & G Boggs (eds), *Mine Closure 2024: Proceedings of the 17th International Conference on Mine Closure*, Australian Centre for Geomechanics, Perth, pp. 1311–1320, https://doi.org/10.36487/ACG_repo/2415_95

Russell, WA, Papanastassiou, DA & Tombrello, TA 1978, 'Ca isotope fractionation on the Earth and other solar system materials', *Geochimica et Cosmochimica Acta*, vol. 42, pp. 1075–1090, https://doi.org/10.1016/0016-7037(78)90105-9

Steiger, RH & Jäger, E 1977, 'Subcommission on geochronology: Convention on the use of decay constants in geo- and cosmochronology', *Earth and Planetary Science Letters*, vol. 36, pp. 359–362, https://doi.org/10.1016/0012-821X(77)90060-7

Tuvdendorj A, Sanjdorj S & Ulziibayar G 2008, *Report on Groundwater Exploration in the Gunii Khooloi Deposit* (in Mongolian), Open File Report, Ministry of Nature and Environment, Ulaanbaatar, pp. 22–30.